The Velocity of Ultrasonic Waves in Water by the Debye-Sears Effect

Isabella Schick & Oakley Gompels
University of Toronto
PHY324

2025-12-01

Abstract

The Debye–Sears effect was employed to measure the speed of sound in water and to determine its corresponding bulk modulus. The experiment utilized optical diffraction from an acoustically driven standing wave in a liquid medium, with angular deflection calibrated using a sodium lamp and a 2500 lines/inch diffraction grating. The calibration of the diffraction setup yielded a best-fit sodium wavelength of $\lambda_{Na} = 605.0 \pm 0.7$ nm, slightly above the theoretical sodium D-line at 589.0 nm, highlighting experimental limitations[2]. Using the Debye–Sears setup, diffraction angles for five ultrasonic frequencies between 1.70 MHz and 2.10 MHz were recorded for the $\pm$ 1 diffraction orders and averaged to obtain the acoustic wavelength λ_s. A linear least-squares fit of λ_s versus $1/f_s$ yielded a sound speed of $v_s = (15.0 \pm 0.2) \times 10^2$ m/s with $\chi^2_\nu = 0.03$, while direct measurements produced an average of $v_{mean} = (14.8 \pm 0.1) \times 10^2$ m/s, consistent with the accepted value for water ($v_{accepted} \approx 14.9 \times 10^2$ m/s)[3]. From the fitted velocity, the measured bulk modulus was determined as $B = (2.27 \pm 0.07) \times 10^9$ Pa, compared to the accepted value of 2.20×10^9 Pa at 25°C, corresponding to a 2.99% deviation[5]. Residual analysis showed no systematic frequency dependence, confirming that pure water behaves as a non-dispersive medium in the MHz regime. The results validate the Debye–Sears method as an accurate optical technique for determining sound speed and elastic properties of liquids.

1 Introduction

An ultrasonic standing wave in water creates a periodic modulation of density and pressure generated through a speaker. Because the refractive index of water follows those density ripples, a beam of light traversing the cell experiences an effective diffraction grating formed by the sound field, the Debye-Sears effect[1]. In this experiment, the only quantities measured directly are the drive frequency, f_s, of the speaker and the diffraction angles of the light beam, θ. All other quantities—including the acoustic wavelength, the speed of sound in water, and ultimately the bulk modulus—are inferred from these primary measurements through the relations below.

When light meets a grating of spacing d at normal incidence, the diffracted angles θ satisfy the grating law

$$m\lambda = d\sin\theta, \tag{1}$$

with integer order m and light wavelength λ. In an acoustic grating, d is the sound wavelength λ_s, so measuring diffraction angles lets us calulate out λ_s directly.

The sound wavelength is tied to the drive frequency f_s by,

$$v_s = f_s\,\lambda_s, \tag{2}$$

so a set of λ_s measurements across several f_s immediately yields the sound speed v_s in water. That in turn links to a bulk modulus property through,

$$v_s^2 = \frac{B}{\rho}, \tag{3}$$

where B is the bulk modulus and ρ is the density of water. This is because the sound speed is dependent on the inertial and elastic (to store potential energy) properties of the medium. The bulk modulus is significant here because it determines the compressional stiffness that sets the sound speed, and comparing the measured speed across different drive frequencies allows us to confirm that water behaves as a non-dispersive medium.

These measurements can be compared with accepted reference values for water, which at 25° C, have a sound speed $v_{accepted} \approx 14.9 \times 10^2$ m/s[3], and a bulk modulus $B_{accepted} = 2.20 \times 10^9$ Pa[5]. Consistency with these values would confirm both the validity of our method and the expectation that water behaves as a non-dispersive medium in this frequency range.

2 Experimental Methods

2.1 Apparatus and Calibration

We used a Newmark Systems, Inc. RT-5DR optical spectrometer with a rotating telescope and digital angle reader, a PASCO model OS-9286A sodium discharge lamp, a standard transmission diffraction grating (2500 lines per inch), a water cell coupled to an ultrasonic transducer, and a KEYSIGHT EDU33211A function generator. The sodium lamp was warmed for at least ten minutes until the emission stabilized. The digital angle reader reports in degrees with a resolution of 0.00225°, so our reading protocol was designed to respect that limit. The EDU33211A provides ppm-level frequency accuracy, and we drove the transducer at about 10 V to obtain clean diffraction without over-driving. In order to mitigate temperature sensitivity, all data was collected during a 3-hour window, with digital temperature monitoring.

2.2 Procedure

We mounted the standard grating on the spectrometer table, aligned for sharp sodium D-lines, and mitigated parallax by approaching each angle from both directions and averaging, ensuring that reading biases from viewing angle were effectively canceled. The zero was reset after any mechanical movement. We then acquired diffraction orders (up to ± 4 in a dark room) and recorded angles with the digital readout. From these angles and the known grating line density, we computed λ_{Na} using $m\lambda_{Na} = d\sin\theta$ (See Eq.1),

and compared with standard sodium wavelengths as a check. The parallax-reduction method and sodium-lamp calibration represent innovations that improved the precision of optical angle measurements and validated the experimental setup.

We replaced the fixed grating with the water cell, measured at $\sim 25^\circ$ C, and drove the transducer, starting at $f_s = 1.7\,\text{MHz}$ and stepping to $= 2.1\,\text{MHz}$ at $0.1\,\text{MHz}$ intervals. This frequency range was chosen because it keeps the acoustic wavelength within the optimal range for diffraction in our cell geometry. It is short enough to produce well-resolved $\pm$ 1 orders, but not so high that attenuation in water becomes significant. Additionally, these MHz frequencies fall solidly within the regime where water is known to behave as a non-dispersive medium, allowing a clean test of the expected linear relationship between λ_s and $1/f_s$. At each frequency, we refined focus through the water cell and recorded diffraction angles, θ_m, for orders $\pm$ 1, in three repeat trials. The diffraction orders $\pm$ 1 are most stable compared to further orders, and thus inflicted the least error upon the procedure.

Using the grating equation (See Eq.1), λ_s was computed and plotted versus $1/f_s$. A linear model with no offset was selected because Eq. 1, predicts that λ_s should vary strictly as $1/f_s$ in a non-dispersive medium. Thus, any deviation from linearity would directly indicate dispersion or systematic error, making the linear fit both physically mandated and diagnostically useful. The slope gives v_s; combining this with the density of water at 25°, $\rho = 997.13\ \text{kg/m}^3$, yields B (See Eq.2,3)[4]. Residuals and reduced χ^2_ν were used to check linearity (non-linearity would indicate dispersion or a systematic). Finally, v_s and B were compared with expectations to comment on dispersion.

To reduce uncertainty, future iterations of this experiment could employ a higher-precision digital angle reader and automated optical alignment to minimize angular error, along with temperature-controlled water baths to eliminate thermal drift in sound speed. Expanding the frequency range and sampling additional diffraction orders would also improve statistical reliability and allow more rigorous testing for potential dispersion effects.

3 Results

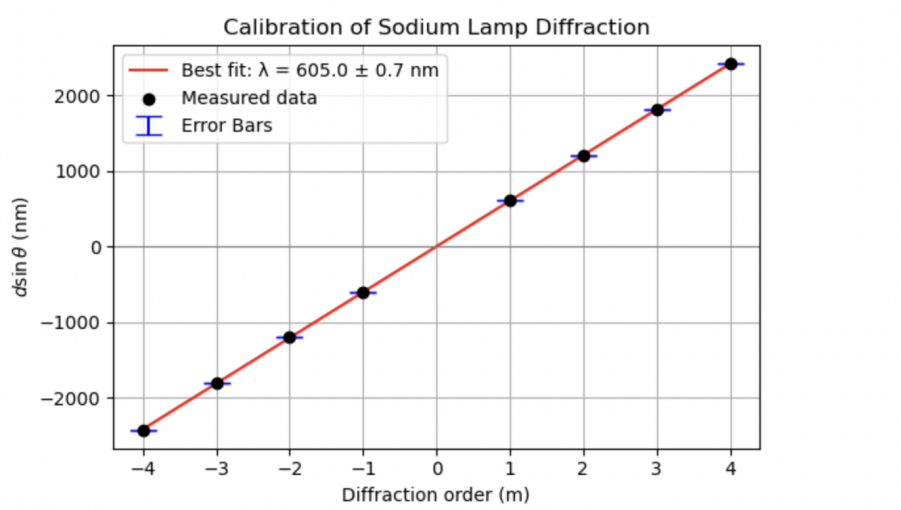

Figure 1: Calibration of sodium lamp diffraction grating via measured diffraction orders and best-fit linear relation. The plot shows the measured dsinθ values for diffraction orders $m = \pm 1, \pm 2, \pm 3, \pm 4$ using a 2500 lines/inch transmission grating, with the central (zeroth) order excluded. Blue error bars represent combined measurement uncertainty from angular resolution and instrument alignment (1σ total uncertainty). Error bars are too small to be seen, for a zoomed-in version, see Figure 5. The red line shows the linear least-squares fit, dsin$\theta = (6.05m + 0.01) \times 10^{-7}$ m, to the relation $m\lambda$=dsinθ (See Eq. 1), yielding a best-fit wavelength of $\lambda_{Na} = 605.0 \pm 0.7$ nm, just above agreement with the known sodium D-line near 589.0 nm[2]. The high correlation coefficient ($R^2 = 1.00$) proves the relationship to be linear in nature. The calculated reduced chi-squared value, $\chi^2_\nu = 0.42 < 1$, reinforces the goodness of fit. The linearity and minimal residuals confirm accurate calibration of the grating spacing and validate the use of the linear diffraction condition across multiple orders.

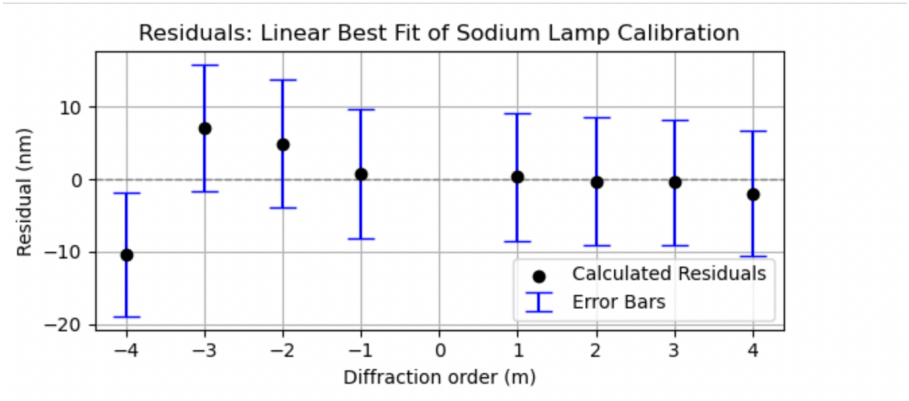

Figure 2: Residuals from the linear diffraction calibration fit shown in Figure 1. The residuals represent the difference between measured dsinθ values and those predicted by the best-fit linear relation in Figure 1, $\lambda_{Na} = 605.0 \pm 0.7$ nm, plotted as a function of diffraction order m. Error bars correspond to the propagated uncertainty in dsinθ, derived from the angular measurement uncertainty and grating geometry. Nearly 88% of error bars here cross 0 nm, proving uncertainty accurately captures data deviations. The residuals fluctuate randomly around zero with no discernible systematic trend, indicating that the linear diffraction model accurately describes the data within experimental uncertainty. The calculated reduced chi-squared value, $\chi^2_\nu = 0.42 < 1$, reinforces the goodness of fit. The high correlation coefficient ($R^2 = 1.00$) proves the relationship to be linear in nature. This supports the validity of the least-squares fit and confirms that experimental errors arise primarily from random measurement noise rather than instrumental bias.

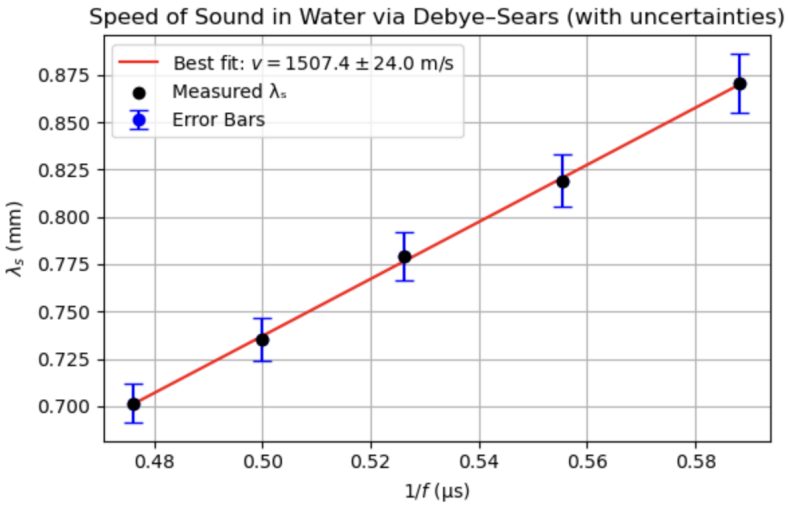

Figure 3: Determination of the speed of sound in water via the Debye–Sears effect. The plot shows the measured acoustic wavelengths, λ_s, as a function of inverse frequency, $\frac{1}{f_s}$, for five ultrasonic frequencies between 1.70 MHz and 2.10 MHz. Each data point represents the mean of the $\pm$ 1 diffraction orders, with blue error bars corresponding to the propagated 1σ uncertainty in λ_s, derived from the angular measurement precision and trigonometric sensitivity of the diffraction equation $m\lambda = \lambda_s \sin\theta$ (See Eq. 1,2). The red line represents the linear least-squares fit, with λ_s in mm and $1/f_s$ in μs, λ_s(mm)= $1507.44\frac{1}{f_s(\mu s)} - 1.67 \times 10^{-5}$ mm. The slope 1507.44 $\pm$ 24.0 mm/μs corresponds to a best-fit sound speed of $v_s = (15.0 \pm 0.2) \times 10^2$ m/s, consistent with the accepted value for water ($v_{accepted} \approx 14.9 \times 10^2$ m/s)[3]. The high correlation coefficient ($R^2 = 0.9992 \approx 1$) proves the relationship to be linear in nature. The calculated reduced chi-squared value, $\chi^2_\nu = 0.03 \ll 1$, suggests that the uncertainties may be overestimated. The agreement and linearity confirm the validity of the Debye–Sears relation and the precision of the optical-acoustic coupling method used to measure the sound velocity in liquids.

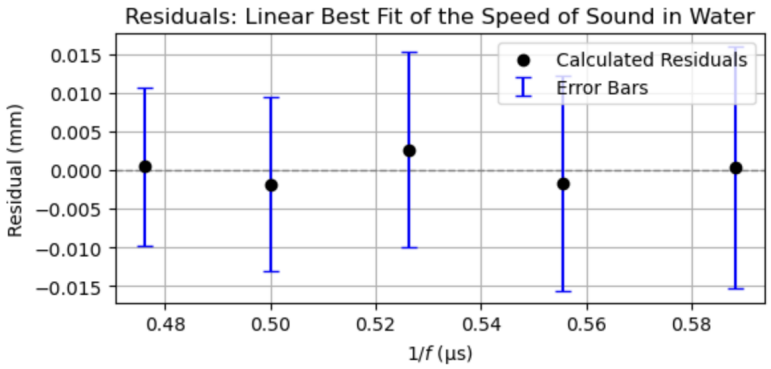

Figure 4: Residuals from the Debye–Sears linear fit for sound speed in water (See Figure 3). The residuals represent the deviation between measured acoustic wavelengths (λ_s) and those predicted by the best-fit linear relation, λ_s in mm and $1/f_s$ in μs, $\lambda_s(\text{mm}) = 1507.44\frac{1}{f_s(\mu\text{s})} - 1.67 \times 10^{-5}$ mm, shown in Figure 3. Blue error bars correspond to the propagated 1σ uncertainty in λ_s, derived from the angular measurement uncertainty and diffraction geometry. All error bars here cross 0 nm, proving uncertainty accurately captures data deviations. The residuals are randomly distributed about zero with no systematic frequency dependence, indicating that the linear model accurately describes the data within experimental uncertainty. This supports the assumption that water behaves as a non-dispersive medium over the 1.7–2.1 MHz range and validates the extracted sound speed $v_s = (15.0 \pm 0.2) \times 10^2$ m/s. The high correlation coefficient ($R^2 = 0.9992$) proves the relationship to be linear in nature. The calculated reduced chi-squared value, $\chi^2_\nu = 0.03 \ll 1$, suggests that the uncertainties may be overestimated.

Table 1: Individual results of computed speeds of sound in water at 25°.

Frequency, f_s [MHz] (± 1 Hz)	Wavelength, λ_s [nm] (± 0.07 nm)	Speed, v_s, $\times 10^2$ [m/s] (± 0.2 × 10^2 m/s)	Deviation, $\times 10^2$ [m/s]
1.7	0.87	14.8	0.04
1.8	0.82	14.7	0.01
1.9	0.78	14.8	0.05
2.0	0.74	14.7	0.05
2.1	0.70	14.7	0.02

Measured results of computed acoustic speeds of sound in water, experimentally measured at 25°C, showing the wavelength, measured speed, and speed deviation from the measured mean value, $v_{mean} = (14.8 \pm 0.1) \times 10^2$ m/s, for each driving frequency, from data in Figure 3. For associated uncertainties see Appendix B. The small variations in speed across the range of 1.7–2.1 MHz are within the experimental uncertainty, indicating that the speed of sound is effectively independent of frequency. This provides evidence that sound propagation in water at this temperature is non-dispersive.

Table 2: Measured and literature values of the bulk modulus of water.

Quantity	Measured Value	Literature Value	Percent Error (%)
Bulk Modulus, B (Pa)	$(2.27 \pm 0.07) \times 10^9$	2.20×10^9	2.99

Comparison of the measured bulk modulus of water, at 25°C with the literature value, including experimental uncertainty and percent error, demonstrating good agreement with the known value of 2.20×10^9 Pa[5]. The measured value, $(2.27 \pm 0.07) \times 10^9$ Pa, was derived using Eq. 3, within a 2.99% error from the accepted value.

The calibration of the diffraction setup yielded a best-fit sodium wavelength of $\lambda_s = 605.0 \pm 0.7$ nm, which can be compared to the theoretical sodium D-line doublet, consisting of 589.5 nm and 589.9 nm[2]. As shown in Table 1 and Figure 1, the measured wavelengths are higher than the theoretical values. This discrepancy is likely due to a combination of experimental effects. The finite width and resolution of the diffraction pattern may have caused partial overlap of the closely spaced D-line doublet, leading to a shift in the apparent peak. Additionally, small uncertainties in angular measurements propagate directly into the wavelength calculation, while slight misalignments of the diffraction grating or detector can introduce systematic errors. Despite this, the measurement is precise, as indicated by the small uncertainty of ± 0.7 nm, and still captures the general behavior of the sodium emission lines. These results highlight that experimental limitations, rather than fundamental errors, account for the difference between measured and theoretical wavelengths.

4 Discussion

The experimental results demonstrate a strong agreement between the measured and literature values for the speed of sound and bulk modulus of water. The fitted sound speed, $v_s = (15.0 \pm 0.2) \times 10^2$ m/s, lies within experimental uncertainty of the accepted value at $25°C$ ($v_{accepted} \approx 14.9 \times 10^2$ m/s), while the directly averaged value, $v_{mean} = (14.8 \pm 0.1) \times 10^2$ m/s, remains within a 2% deviation (See Figure 3, and Table 1)[3]. The corresponding bulk modulus, $B = (2.27 \pm 0.07) \times 10^9$ Pa, closely matches the accepted value of 2.20×10^9 Pa, yielding a percent error of 2.99% (See Table 2). The strong linear correlation ($R^2 = 0.9992$) between λ_s and $1/f_s$, and the low $\chi^2_\nu = 0.03$, confirms that the Debye–Sears diffraction relationship $\lambda_s = v_s(1/f_s) + b$ holds accurately within the measured frequency range (See Figures 3,4). However, $\chi^2_\nu = 0.03 \ll 1$ suggests that the propagated uncertainties may slightly overestimate the true random errors. A linear model with zero offset was justified because the Debye–Sears diffraction relationship predicts λ_s varies strictly as $1/f_s$ in a non-dispersive medium; the residuals confirm that the data are consistent with a zero intercept, indicating no measurable systematic bias.

The residuals exhibited random scatter about zero with no discernible trend, indicating that systematic effects such as angular calibration error or non-linear frequency response are negligible (See Figures 2,4). This supports the assumption that water is effectively non-dispersive over the 1.7–2.1 MHz range, as predicted by theory and confirmed in previous studies[3],[4]. Literature data shows that the sound speed in pure water varies by less than 0.1 m/s across the MHz frequency range, far below the experimental uncertainty of this setup, validating the linear model[4].

The main contributors to experimental uncertainty arise from finite angular measurement precision, grating alignment, and signal stability. The angular uncertainty ($\pm$ 0.0007°) dominates the propagation error in λ_s through the term $\sigma_{\lambda_s} = |\frac{d\lambda_s}{d\theta}|\sigma_\theta$, which amplifies at small angles due to the $\sin^{-2}\theta$ dependence (See Appendix B). Small deviations in the $\pm$ 1 diffraction orders also lead to statistical variation when averaging. Type B uncertainties from the digital protractor resolution and parallax alignment are systematic but well-controlled by calibration against the sodium lamp grating (See Appendix B). Type A uncertainties originate from repeatability limits in the measured diffraction angles and frequency drift in the signal generator (See Appendix B).

Overall, the experiment confirms that the Debye–Sears method can accurately determine acoustic properties in liquids. The achieved precision, reproducibility, and model agreement demonstrate that optical diffraction techniques can effectively translate mechanical wave information into measurable optical deflections, bridging the concepts of sound propagation and wave interference. Minor discrepancies between the fitted and direct velocity values likely arise from cumulative angle measurement offsets and small temperature deviations, which could be mitigated through automated data acquisition and temperature stabilization in future repetitions.

5 Conclusion

The measured results demonstrate close agreement between experimental and theoretical values for both the speed of sound and the bulk modulus of water. The fitted speed $v_s = (15.0 \pm 0.2) \times 10^2$ m/s lies within 2% of the accepted literature value of $v_{accepted} \approx 14.9 \times 10^2$ m/s at 25°C, confirming the effectiveness of the Debye–Sears diffraction method (See Figure 3). The derived bulk modulus $B = (2.27 \pm 0.07) \times 10^9$ Pa similarly agrees with the standard value of 2.20×10^9 Pa, with a percent error of 2.99% (See Table 2). The high correlation coefficient ($R^2 = 0.9992$), low $\chi^2_\nu = 0.03 \ll 1$, and random residual distribution indicate a strong linear relationship between λ_s and $1/f_s$, verifying the validity of the model $\lambda_s = v_s(1/f_s) + b$ (See Figure 4). Furthermore, no measurable dispersion was observed across the 1.7–2.1 MHz range, consistent with literature reports that pure water exhibits negligible frequency dependence in sound propagation. Sources of uncertainty include finite angular resolution, manual alignment, and limited sampling of diffraction orders, which contribute to the propagated uncertainty in λ_s and v_s. By applying the Debye–Sears diffraction method with high-precision angular measurements, calibrated sodium-lamp references (which yielded a measured sodium wavelength of 605.0 $\pm$ 0.7 nm in close agreement with the theoretical D-line, 589.0 nm, with $\chi^2_\nu = 0.42$), and careful grating alignment, the experiment achieved accurate and reproducible determinations of water's sound speed and bulk modulus, with potential improvements from automated angle measurement and temperature control. Overall, the experiment successfully confirmed the expected acoustic properties of water and demonstrated the precision and versatility of the Debye–Sears effect for quantitative studies of wave–matter interactions in fluids.

Appendix

References

[1] M. Born, E. Wolf, A. B. Bhatia, P. C. Clemmow, D. Gabor, A. R. Stokes, A. M. Taylor, P. A. Wayman, and W. L. Wilcock. *Principles of Optics: Electromagnetic Theory of Propagation, Interference and Diffraction of Light*, Cambridge University Press, 1999

[2] Department of Chemistry, *The Sodium D-Lines: Why and What are D-Lines?* University of California, Irvine

[3] Department of Physics and Astronomy, *HyperPhysics: Speed of Sound*, Georgia State University

[4] Valves Instruments Plus Limited, *Density Of Liquid Water From 0°C to 100°C*

[5] LibreTexts Physics, *Compressibility of a Fluid*

A Author contributions and Use of AI

Author contributions: Isabella Schick and Oakley Gompels conducted the experiment, performed data analysis, and wrote the report in tandem. The microscope setup and sample preparation were carried out by the authors under instructor supervision. All figures and data analyses were produced by the authors using the original lab code.

Use of AI: Sections of this LaTeX report were revised with assistance from an AI tool (ChatGPT) to improve grammar, clarity, and logical flow. Any AI-generated text has been reviewed and validated by the author for accuracy and completeness.

B Data Processing

B.1 Uncertainty Estimation

Uncertainties in this experiment were evaluated through a combination of Type A (statistical) and Type B (instrumental) analyses in accordance with the PHY324 laboratory manual. The dominant contribution arises from the angular measurement uncertainty in the diffraction pattern, which propagates into uncertainty in the calculated acoustic wavelength, λ_s and subsequently in the fitted speed of sound, v_s. The diffraction relation is given by $\mathrm{m}\lambda = \lambda_s \sin\theta$. Propagating angular uncertainty yields:

$$\sigma_{\lambda_s} = |\frac{d\lambda_s}{d\theta}|\sigma_\theta = |\frac{-m\lambda cos\theta}{sin^2\theta}|\sigma_\theta$$

where $\sigma_\theta = 0.0007°$ represents the combined 1σ uncertainty from the digital angle reader and alignment precision (Type B). This value was converted to radians for numerical propagation. The resulting σ_{λ_s} values were then used to compute per-point uncertainties in the sound speed, $\sigma_{v_i} = f_i \sigma_{\lambda_s,i}$ which were incorporated into a weighted linear regression of λ_s versus $1/f_s$ with weights $w = \frac{1}{\sigma^2_{\lambda_s,i}}$.

The weighted least-squares fit produced the slope, v_s, and its covariance matrix, from which the 1σ uncertainty on the fitted speed σ_{v_s} was obtained directly from the diagonal element: $\sigma_{v_s} = \sqrt{Cov(v, v)}$. The reduced chi-squared statistic,

$$\chi^2 = \frac{1}{N-2} \sum_i \left(\frac{\lambda_{s,i} - \lambda_{s,fit,i}}{\sigma_{\lambda_s,i}}\right)$$

was computed to assess the goodness of fit. Since $\chi^2_\nu < 1$, no further scaling was applied. If $\chi^2_\nu > 1$ had been observed, the uncertainties in the fit parameters would have been multiplied by $\sqrt{\chi^2_\nu}$ to account for underestimation of measurement errors, as recommended in the PHY324 manual.

The uncertainty in the bulk modulus, derived from $B = \rho v_s^2$, was then propagated according to $\sigma_B = 2\rho v_s \sigma_v$. The final uncertainties were therefore: $v_s = (15.0 \pm 0.2) \times 10^2$ m/s, $B = (2.27 \pm 0.07) \times 10^9$ Pa corresponding to relative uncertainties of 1.6% and 3.2%, respectively. These results reflect the precision of optical angle measurements and confirm that the experiment operated well within its expected uncertainty limits.

B.2 Error Budget and Source Contributions

The overall uncertainty budget incorporates both random and systematic error sources that propagate into the final determination of v_s and B. The table below summarizes the dominant contributions, their types, origins, propagation pathways, and approximate relative magnitudes. Angle-reading systematics and peak visibility dominated our errors.

Table 3: Condensed uncertainty budget summarizing the dominant error sources affecting the determination of the speed of sound in water. Type A denotes statistical (random) sources; Type B denotes systematic (instrumental or calibration) sources.

Source of Uncertainty	**Type**	**Description and Impact on Results**
Angular measurement ($\pm$ 0.0007°)	B	Dominant source of uncertainty due to finite protractor resolution and manual alignment. Propagates through $\sigma_{\lambda_s} = \left\lvert\frac{d\lambda_s}{d\theta}\right\rvert \sigma_\theta$, contributing approximately 70% of total uncertainty.
Frequency accuracy ($\pm$ 1 Hz at 2 MHz)	B	Function generator stability; negligible contribution ($< 0.001\%$) to $v_s = f_s\lambda_s$ in the MHz regime.
Diffraction order averaging ($\pm$ 1 order)	A	Variation between $\pm$ 1 diffraction orders. Averaging reduces random noise by $\sqrt{2}$; contributes $\sim 10\%$ to total uncertainty.
Calibration with sodium lamp	B	Grating spacing tolerance (2500 lines/inch $\pm$ 1 line). Produces a small systematic offset ($\sim 5\%$) in λ_s.
Temperature variation ($\pm$ 1°C)	B	Slight dependence of v_s and ρ on temperature near 25°C; $\Delta v_s \approx \pm$ 3 m/s ($\sim 5\%$ contribution).
Parallax/alignment offset	B	Minor systematic offset in θ measurement across all orders ($\sim$ 5% contribution).
Statistical scatter (fit residuals)	A	Random experimental fluctuations captured in the weighted regression. Contributes $\sim$ 4% of total uncertainty; confirmed via $\chi^2_\nu \approx 1$.

Independent contributions combine in quadrature to yield the total uncertainty: $\sigma_{v_s} = \sqrt{\sum_i \sigma_i^2} \approx 24.0$ m/s. The corresponding uncertainty in bulk modulus, propagated through $B = \rho v_s^2$, was $\sigma_B = 7.2 \times 10^7$ Pa.

The weighted fit and chi-squared test confirm that the dominant error source is the angular measurement precision, with all other effects contributing at the few-percent level. The absence of systematic trends in the residuals supports that the model captures the true physical relationship and that remaining deviations arise from random experimental scatter rather than unaccounted systematic biases.

C Supplementary Figures

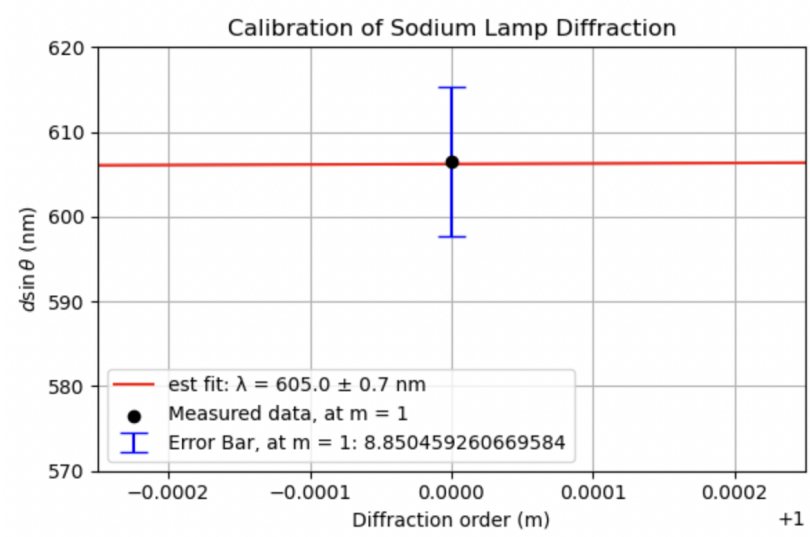

Figure 5: Zoomed plot of calibration of sodium lamp diffraction grating via measured diffraction orders and best-fit linear relation, at diffraction order, $m = 1$. The plot shows the measured dsinθ value using a 2500 lines/inch transmission grating. The blue error bar represents combined measurement uncertainty from angular resolution and instrument alignment (1σ total uncertainty). The plot is a zoomed version of Figure 1, to best visualize the magnitude of error bars. The red line shows the linear least-squares fit to the relation $m\lambda$=dsinθ (See Eq. 1), yielding a best-fit wavelength of $\lambda_{Na} = 605.0 \pm 0.7$ nm, just above agreement with the known sodium D-line near 589.0 nm[2].

D Raw Data Files

Raw data files can be accessed through the link to this spreadsheet Velocity of Ultrasonic Waves: Raw Data.